International Journal of Fatigue 80 (2015) 306–323

Contents lists available at ScienceDirect

International Journal of Fatigue

journal homepage: www.elsevier.com/locate/ijfatigue

A phenomenological stress–strain model for wrought magnesium alloys under elastoplastic strain-controlled variable amplitude loading

Johannes Dallmeier [a,*], Josef Denk [a], Otto Huber [a], Holger Saage [a], Klaus Eigenfeld [b]

[a] *Competence Center for Lightweight Design (LLK), Faculty for Mechanical Engineering, University of Applied Sciences Landshut, Germany*
[b] *Foundry Institute, Technical University Bergakademie Freiberg, Germany*

ARTICLE INFO

Article history:
Received 11 February 2015
Received in revised form 28 May 2015
Accepted 13 June 2015
Available online 24 June 2015

Keywords:
Wrought magnesium alloys
Strain-controlled hysteresis loops
Phenomenological stress–strain model
Variable amplitude loading
Fatigue modelling

ABSTRACT

Wrought magnesium alloys typically reveal strong basal textures and thus, non-symmetric sigmoidal shaped hysteresis loops within the elastoplastic load range. A detailed description of those hysteresis loops is necessary for numerical fatigue analyses. Therefore, a one-dimensional phenomenological model was developed for elastoplastic strain-controlled constant and variable amplitude loading. The phenomenological model consists of a three-component equation, which considers elastic, plastic, and pseudoelastic strain components with a set of eight material constants. Experimentally and numerically determined hysteresis loops of four different magnesium alloys were compared by means of different examples with constant and variable amplitude. Good correlation is reached and the relevant fatigue parameters like strain energy density were estimated with good accuracy. Applying an energy based fatigue parameter on modelled hysteresis loops, the fatigue life is predicted adequately for constant and variable amplitude loading including mean strain and mean stress effects.

1. Introduction

Wrought magnesium alloys possess high potential for lightweight design making them attractive for the automotive industry [1]. The development of an economical twin roll strip casting process for the continuous and semi continuous production of magnesium sheet metals [2,3], e.g. for car body components, was one of the main advancements in the last decade. Magnesium alloys possess a hexagonal close packed crystal structure, indicated in Fig. 1. The most pronounced deformation mechanisms of magnesium single crystals at ambient temperature are basal ⟨a⟩ slip and {10–12}⟨10–11⟩ extension twinning (e.g. [4,5]). A similar behavior was observed for polycrystalline standard alloys such as AZ31, but for some textures and loading directions, the critical resolved shear stress for prismatic ⟨a⟩ slip is exceeded and its portion is large (e.g. [5–7]). Extension twinning is possible at low stresses and enables tensile straining along the *c*-axis [4]. Thus, it can be activated when a tensile stress is applied parallel or a compressive stress is applied perpendicular to the *c*-axis as illustrated in Fig. 1 (e.g. [4]). Wrought magnesium semifinished products exhibit strong textures in contrast to magnesium castings, which typically show a random grain orientation (e.g. [3,4,8]). During sheet metal forming, a basal texture with the *c*-axis lying almost normal to the sheet plane is developed (e.g. [8]), which results in an asymmetry of the tensile and compressive yield stress (e.g. [9]). In the low-cycle fatigue regime, the cyclic plastic deformation is mainly caused by reiterative twinning and detwinning (e.g. [10]) and sigmoidal shaped stress–strain hysteresis loops can be observed (e.g. [8,10]). Moreover, most of the magnesium alloys show a nonlinear unloading curve in the tensile as well as compressive region, which is called pseudoelastic behavior (e.g. [11–13]). In magnesium alloys, pseudoelastic strain is caused by reversible movements of twin boundaries due to internal driving forces [11]. This strain leads to larger hysteresis loops especially at low stress amplitudes in comparison to material behavior without pseudoelasticity [11].

Several strain-controlled evaluations were carried out on wrought magnesium alloys to predict the fatigue life by the local strain concept (e.g. [9,14–30]). A comprehensive summary of fatigue investigations on wrought magnesium alloys is given in [30]. Accordingly, most low-cycle fatigue investigations [9,14–23] were done using completely reversed strain-controlled conditions, and in [24–30] the influence of the strain ratio was considered. The Manson–Coffin–Basquin approach [31–33] was found to show an adequate correlation with the experiments for completely reversed strain-controlled conditions (e.g. [9,15–19,23]). In addition, energy based fatigue models were shown to give good correlation in cases of variable strain or stress ratios [20,22,26,29,30].

---

[*] Corresponding author at: Am Lurzenhof 1, 84036 Landshut, Germany. Tel.: +49 1704726731.

E-mail address: Johannes.Dallmeier@haw-landshut.de (J. Dallmeier).

http://dx.doi.org/10.1016/j.ijfatigue.2015.06.007
0142-1123/© 2015 Elsevier Ltd. All rights reserved.

Nomenclature

a_{down}	shape factor for descending reversals
a_{up}	shape factor for ascending reversals
CYS	compressive yield stress
CSSC	cyclic stress–strain curve
E	Young's modulus
ED	extrusion direction
EL	tensile elongation
K'	cyclic strength coefficient
m_{psel}	memory factor for pseudoelastic strain component
m_{pl}	memory factor for plastic strain component
n'	cyclic strain hardening exponent
N_{b}	number of cycles to break in two pieces
N_{f}	number of cycles to failure
$N_{\mathrm{f,r}}$	remaining number of cycles to failure
$N_{\mathrm{loop,f}}$	number of full loops to failure
P	material constant, representing the slope of the pseudoelastic strain component
P_{SWT}	Smith–Watson–Topper fatigue parameter [58]
RCS	relative coordinate system
RD	rolling direction
R_{r}	ratio between the reduction of both memory factors m_{pl} and m_{psel}
R_{ε}	strain ratio
R_{σ}	stress ratio
S	material constant, representing the slope at the inflection point of the plastic strain component
T	amount of plastic strain at the inflection point of the plastic strain component
TYS	tensile yield stress
U	substitution function
UTS	ultimate tensile strength
Δ	deviation between two compared quantities
ΔW_{comb}	combined strain energy density per cycle
$\Delta W_{\mathrm{comb,ww}}$	combined strain energy density per cycle without weighting
$\Delta W_{\mathrm{el+}}$	tensile elastic strain energy density per cycle
ΔW_{pl}	plastic strain energy density per cycle
$\Delta W_{\mathrm{psel+}}$	positive pseudoelastic strain energy density per cycle
$\Delta\varepsilon_{\mathrm{t}}$	relative total strain for the actual reversal in the actual RCS/total strain range
$\Delta\varepsilon_{\mathrm{el}}$	elastic strain component
$\Delta\varepsilon_{\mathrm{pl}}$	plastic strain component
$\Delta\varepsilon_{\mathrm{psel}}$	pseudoelastic strain component
$\Delta\sigma$	relative stress for the actual reversal in the actual RCS/stress range
$\Delta\sigma_{\mathrm{max}}$	maximum stress range of the envelope hysteresis loop
$\dot{\varepsilon}$	strain rate
ε_{t}	total strain of the initial loading curve, described by the Ramberg–Osgood equation
$\varepsilon_{\mathrm{a,el}}$	elastic strain amplitude
$\varepsilon_{\mathrm{a,pl}}$	plastic strain amplitude
$\varepsilon_{\mathrm{a,pl,m1}}$	plastic strain amplitude for assumed linear elastic unloading (method 1)
$\varepsilon_{\mathrm{a,pl,m2}}$	real plastic strain amplitude, half width of hysteresis loop at $\sigma = 0$ MPa (method 2)
$\varepsilon_{\mathrm{a,pl,m3}}$	half width of hysteresis at the mean stress of the loop (method 3)
$\varepsilon_{\mathrm{a,t}}$	total strain amplitude
σ	stress of the initial loading curve, described by the Ramberg–Osgood equation
σ_{a}	stress amplitude
σ_{dtw}	stress at the inflection point of the plastic strain component of the ascending reversal
σ_{m}	mean stress
σ_{max}	maximum stress
σ_{min}	minimum stress
$\sigma_{\mathrm{p,down}}$	pseudoelastic cut-off stress for descending reversals
$\sigma_{\mathrm{p,up}}$	pseudoelastic cut-off stress for ascending reversals
σ_{rp}	global stress at the beginning of a reversal
σ_{tw}	stress at the inflection point of the plastic strain component of the descending reversal
(e)	engineering stress or strain (used as index)
(t)	true stress or strain (used as index)

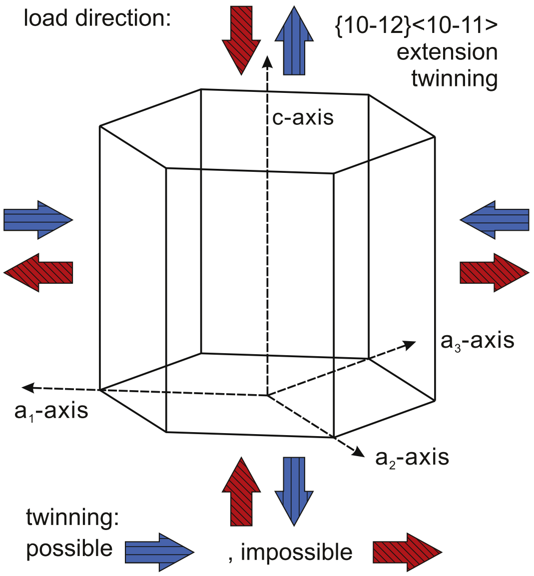

Fig. 1. Direction dependency of {10–12}⟨10–11⟩ twinning.

Zenner and Renner [34] analyzed the shape of hysteresis loops at variable amplitude loading and showed that different magnesium alloys exhibit material memory. Götting and Scholtes [35] investigated the influence of strain-controlled loading history on the stress–strain behavior of AZ31 wrought magnesium alloy and found the shape of the reversals to be strongly influenced by predeformation. The larger the compressive predeformation and thus, the amount of twins, the larger is the deviation from linearity at the beginning of a reversal. It can be seen in both studies [34,35] that the shapes of reversals at variable amplitude loading depend on several parameters such as mean strain, predeformation and strain amplitude. Nevertheless, experimentally determined hysteresis loops were evaluated without consideration of an adequate stress–strain model in [34,35].

Appropriate numerical fatigue analyses require the knowledge of the elastoplastic stress–strain curves of each cycle to provide the required stress, strain, and strain energy density components. In most previous studies, the experimentally determined hysteresis loops were used to obtain the necessary values (e.g. [14–30]), which is not practicable in an engineering fatigue analysis. Therefore, the shape of stress–strain hysteresis loops must be described with an efficient model.

For some steel and aluminum alloys, the Ramberg–Osgood equation [36] in combination with the Masing model [37] is an